JACS
JOURNAL OF THE AMERICAN CHEMICAL SOCIETY
Article
pubs.acs.org/JACS

Real-Time Observation of the Formation of Excited Radical Ions in Bimolecular Photoinduced Charge Separation: Absence of the Marcus Inverted Region Explained

Marius Koch,[†,§] Arnulf Rosspeintner,[†,§] Katrin Adamczyk,[‡,∥] Bernhard Lang,[†] Jens Dreyer,[‡,⊥] Erik T. J. Nibbering,*[,‡] and Eric Vauthey*[,†]

[†]Department of Physical Chemistry, University of Geneva, 30 Quai Ernest-Ansermet, CH-1211 Geneva 4, Switzerland
[‡]Max Born Institut für Nichtlineare Optik und Kurzzeitspektroskopie, Max-Born-Strasse 2A, 12489 Berlin, Germany

Supporting Information

ABSTRACT: Unambiguous evidence for the formation of excited ions upon ultrafast bimolecular photoinduced charge separation is found using a combination of femtosecond time-resolved fluorescence up-conversion, infrared and visible transient absorption spectroscopy. The reaction pathways are tracked by monitoring the vibrational energy redistribution in the product after charge separation and subsequent charge recombination. For moderately exergonic reactions, both donor and acceptor are found to be vibrationally hot, pointing to an even redistribution of the energy dissipated upon charge separation and recombination in both reaction partners. For highly exergonic reactions, the donor is very hot, whereas the acceptor is mostly cold. The asymmetric energy redistribution is due to the formation of the donor cation in an electronic excited state upon charge separation, confirming one of the hypotheses for the absence of the Marcus inverted region in photoinduced bimolecular charge separation processes.

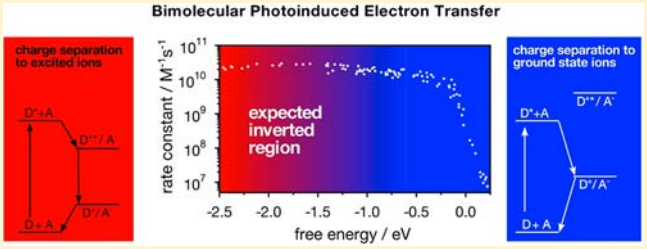

INTRODUCTION

The most striking prediction of Marcus electron-transfer (ET) theory is probably the quadratic free energy dependence of the ET rate constant,[1] in contrast with the Bell−Evans−Polanyi principle that has been, and still is, very successful in physical organic chemistry.[2] The predicted decrease of the rate constant with increasing driving force, the so-called Marcus inverted region,[3] had to wait for more than 20 years to be experimentally observed.[4] Since then, the inverted region has been reported for almost all types of ET reactions: intra- and intermolecular charge shift,[4,6] intra- and intermolecular charge recombination (CR),[7] and intramolecular charge separation (CS).[8] However, so far there still has been no unambiguous report of the inverted region for intermolecular photoinduced CS, i.e., for bimolecular ET quenching processes.[9] Indeed, as shown by Rehm and Weller more than 40 years ago,[5b,10] the quenching rate constant first increases with driving force until it becomes equal to the diffusion rate constant and then remains essentially unchanged even for driving forces larger than 2.5 eV (Figure 1). Various hypotheses have been proposed to account for the strong deviation from Marcus theory for this type of ET: (i) electronically excited ions as the primary CS product,[5b,11] (ii) an increase of the ET distance with increasing driving force;[5c,12] (iii) a breakdown of the linear response of the solvent polarization.[13] Whereas there are several indications that the linear response of the solvent is an adequate assumption for ET processes between organic molecules,[14] none of the other two

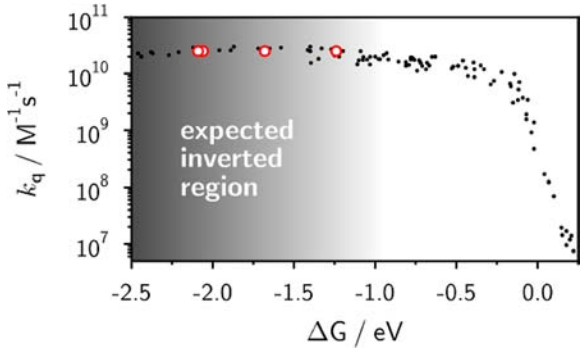

Figure 1. Driving force dependence of the stationary quenching rate constant, k_q, of bimolecular fluorescence quenching measured with the four D/A pairs investigated here (red) and comparison with literature values (from ref 5).

hypotheses could be confirmed or refuted so far.[15] The participation of excited ions would decrease the effective driving force, while remote ET would shift the inverted region to higher driving forces. Therefore, the ability of the remote ET model of reproducing the observed driving force dependence of the quenching rate does not rule out the hypothesis of a reaction pathway via excited ions.

Received: April 8, 2013
Published: June 10, 2013

 © 2013 American Chemical Society dx.doi.org/10.1021/ja403481v | J. Am. Chem. Soc. 2013, 135, 9843−9848

The formation of the ET product in an electronic excited state has already been observed, but for other types of charge-transfer processes. It is at the origin of electrochemiluminescence,[16] and it has also been found upon CR of geminate ion pairs.[17] In the latter case, the presence of an energetically accessible electronic excited state of the product has been shown to lead to ultrafast CR and to suppress the Marcus inverted regime. Such an excited product pathway can be expected to be operative for photoinduced CS as well. Unfortunately, excited radical ions are extremely difficult to detect at room temperature because of their very short lifetimes, typically a few hundreds of femtoseconds to a few picoseconds.[18] Moreover, none of these species investigated so far exhibit very distinct spectral signatures that would allow identification of their fugacious presence in a bimolecular photoinduced CS process.[18e]

Here we present unambiguous evidence of the participation of excited radical ions in strongly exergonic bimolecular photoinduced CS. Combining femtosecond time-resolved emission and transient mid-IR and visible absorption spectroscopy allows us to follow the pathways of energy dissipation during the CS−CR cycle. The results presented here finally give an answer to the long-lasting question about the non-observation of the inverted region for photoinduced bimolecular CS. The absence is not due to a failure of Marcus theory but rather due to the difficulty to identify the primary product of highly exergonic ET reactions.

PRINCIPLE OF THE EXPERIMENT

The general idea of the experiment is as follows: In the CS−CR cycle, the entire excitation energy is eventually converted into heat. However, the initial distribution of vibrational energy over the reaction product depends on whether the primary CS product is excited (CS*) or not (CS°) (Figure 2). When the

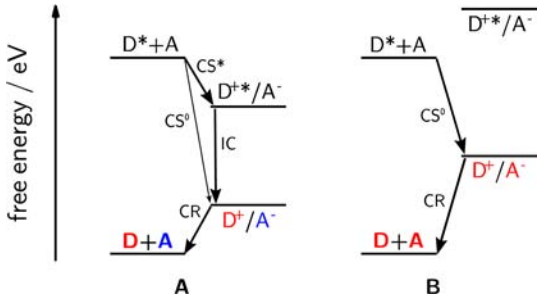

Figure 2. Electronic energy diagrams describing the two possibilities for photoinduced charge separation and recombination for the D/A systems investigated. Red and blue denote vibrationally hot and cold species, respectively.

overall cycle is substantially faster than thermal equilibration, it is experimentally possible to observe, within the first picoseconds after photoexcitation, the vibrationally hot neutral ground-state population. The absorption band shape of this population provides quantitative information on the energy release, thus on whether CS° or CS* is operative.

The four donor/acceptor (D/A) pairs investigated here are structurally very similar and consist of either 9,10-dicyanoanthracene (DCA), 3-cyanoperylene (CNPe), 9,10-diphenylanthracene (DPA), or 3-methylperylene (MePe) as donor and tetracyanoethylene (TCNE) as acceptor (Chart 1). These four pairs have been chosen such that CS* gradually changes from

Chart 1. Structures of the Electron Donors and Acceptor

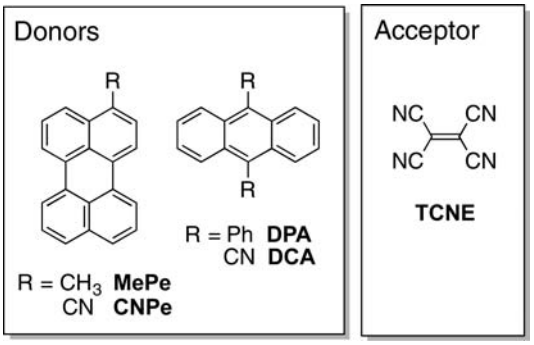

endergonic to moderately exergonic. At the same time, CS° gradually changes from moderately to highly exergonic. The first electronic excited state of $TCNE^{\bullet-}$ is much higher ($E_{00}(A^{\bullet-})$ = 2.6 eV)[21] than that of all four donor radical cations (Table 1), and therefore its population upon CS* can be

Table 1. Energetic Parameters for Photoinduced CS with the Donor/TCNE Pairs in Acetonitrile[a]

donor	E_{00} (D) (eV)	E_{ox}(D) V vs SCE	$E_{00}(D^+)$ (eV)	$\Delta G_{CS°}$ (eV)	ΔG_{CS*} (eV)
DCA	2.89	1.89[c]	1.54	−1.24	+0.30
CNPe	2.65	1.21	1.26	−1.68	−0.42
DPA	3.09	1.27[b]	1.35	−2.06	−0.71
MePe	2.83	1.00	1.45	−2.07	−0.63

[a]Using E_{red}(TCNE) = 0.24 V vs SCE; ref 5b. [b]Ref 19. [c]Ref 20.

disregarded. As shown in Figure 1, the stationary quenching of all four donors by TCNE in acetonitrile is diffusion controlled,[20] even though quenching of DPA and MePe would be expected to be in the inverted region.

Upon 400 nm excitation, ∼3.1 eV are deposited in the donor as electronic, E_{00}, and vibrational energy. Upon CS and CR back to the neutral ground state, this energy is eventually entirely dissipated as heat. The energy associated with the solvent reorganization is directly transferred into the environment, whereas the remainder is transformed into vibrational energy of the reaction partners, before being eventually dissipated into the environment via vibrational cooling. If both CR and CS take place on a time scale much faster than vibrational cooling, then the final neutral product may reach a very high vibrational temperature. For example, upon excitation of the DCA/TCNE pair at 400 nm, about 0.21 eV excess energy is transferred into DCA vibrations, and, upon CS° and CR, 2.89 eV is converted into excitations of solvent and vibrational modes of DCA and TCNE. Assuming that only half of this energy is channelled to vibrational modes of the reaction products leads to a vibrational temperature of DCA and TCNE of 690 and 640 K, respectively (see Supporting Information for details). In contrast, the final vibrational temperature of the MePe/TCNE pair depends on whether or not the primary CS product is in an electronic excited state. In the former case, the electronic energy of the MePe radical cation, i.e., 1.45 eV, is converted into vibrational energy of MePe only, whereas, in the latter case, the whole CS and CR energy goes into solvent and intramolecular modes of both reaction partners. As a consequence, the vibrational temperatures of MePe and TCNE are 810 and 460 K in the first case and 640 and 590 K in the second. These examples show that, if CS produces the

dx.doi.org/10.1021/ja403481v | J. Am. Chem. Soc. 2013, 135, 9843−9848

ions in the ground state, both MePe and TCNE reach approximately the same final vibrational temperature. On the other hand, if CS produces an excited donor cation, more energy goes in vibrations of MePe, which reaches a much higher final vibrational temperature than TCNE. Therefore, the vibrational temperatures of the reaction partners at the end of the photocycle directly reflect the CS pathway. Since vibrational cooling occurs on time scales ranging from a few up to a few tens of picoseconds,[22] and, as the overall CS and CR photocycle requires typically 5−10 ps,[7e,23] part of the energy initially deposited into vibrational modes leaks out to the solvent before the ground state is fully repopulated. However, as the vibrational cooling dynamics can be reasonably expected to be very similar for the four D/A pairs, the residual temperature still reflects the different CS pathways. A vibrational temperature can only be defined if the population of the vibrational states follows a Boltzmann distribution. This requires that intramolecular vibrational energy redistribution is complete before vibrational cooling starts, a condition that may not be always fulfilled, as revealed by recent investigations.[22d,24] For this reason, we did not attempt to determine the vibrational temperature of D and A after the photocycle but have only compared the relative amount of heat deposited into D and A for the four pairs.

RESULTS AND DISCUSSION

The relative amount of energy deposited upon CS and CR has been deduced from the transient absorption spectra of the four D/A pairs in the IR and visible spectral regions upon 400 nm excitation using 1 M TCNE in acetonitrile (ACN). At this concentration, fluorescence quenching occurs partially in the static and transient regimes.[25] Therefore, the precise CS dynamics has been monitored by fluorescence up-conversion (Figure S4).

Figure 3 shows transient IR absorption spectra measured with the four D/A pairs in the asymmetric C≡N stretch region. The S_1 state of both CNPe and DCA exhibits a broad C≡N stretch band at 2157 cm^{-1} that has been subtracted from the spectra depicted in Figure 3 (see the Supporting Information for the details of the procedure). The remaining features are the two positive bands around 2147 and 2185 cm^{-1} due to the C≡N stretch of $TCNE^{\bullet-}$ radical anion,[26] and a negative bleach around 2199 cm^{-1}, corresponding to the C≡N stretch of TCNE. The small temporal frequency upshift of the positive bands is not related to solvation, that occurs on a subpicosecond time scale in ACN,[27] but is due to the presence of tight and loose ion pairs, which are characterized by different formation and decay dynamics, as discussed in detail in ref 26b. However, at the TCNE concentration used here (1 M), CS results mostly to the formation of tight ion pairs that undergo ultrafast CR. For all four systems, the rise of the $TCNE^{\bullet-}$ bands upon CS occurs within the first picosecond. On the other hand, CR is multiphasic with >90% of the ion pair population, generated upon static quenching, decaying in <10 ps, and the remaining fraction of ion pairs, formed upon diffusional quenching, decaying on a longer time scale.[11d,26b] The most striking difference between the spectra shown in Figure 3 can be seen in the bleach of the neutral TCNE, which is very weak with MePe/TCNE and has essentially vanished after 10 ps and which is much more marked and still clearly visible after 30 ps with the other donors. Moreover, whereas with MePe the maximum of the 2185 cm^{-1} band is independent of time, it exhibits a time-dependent frequency upshift with DCA, CNPe,

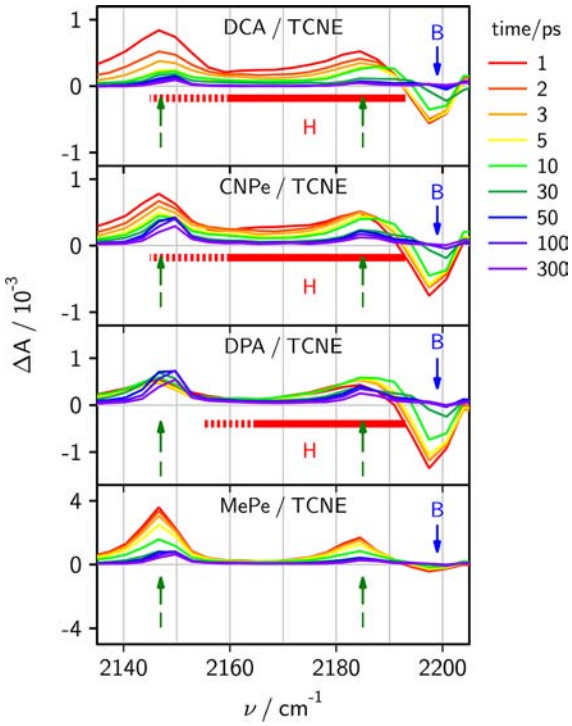

Figure 3. Transient IR absorption spectra in the C≡N stretch region measured with the four D/A pairs at different time delays after 400 nm excitation in acetonitrile (1 M TCNE). The contribution from the excited donor has been subtracted, leaving only the $TCNE^{\bullet-}$ band at ~2147 and 2185 cm^{-1} (I), the TCNE ground-state bleach around 2199 cm^{-1} (B) and hot ground-state features (H). Note that for a proper comparison, the *y*-axes were taken to be symmetric around 0. The different vertical scales are mostly due to dissimilar donor concentrations.

and DPA. This effect can be ascribed to the presence of a hot ground-state absorption band overlapping with the $TCNE^{\bullet-}$ band and shifting to higher frequency as vibrational cooling takes place.

Indeed, the high-frequency IR absorption bands of vibrationally hot molecules are downshifted in frequency with respect to those of cold molecules due to anharmonic coupling with excited low-frequency modes.[28] As a consequence, the spectral signature of a vibrationally hot molecule in a transient IR absorption experiment consists of a negative band, i.e., a bleach, at the vibration frequency of the molecule at room temperature and of a broad positive band at lower frequency (Figure 4).[22b,29] The shape of the induced positive absorption is directly related to the population of excited low-frequency

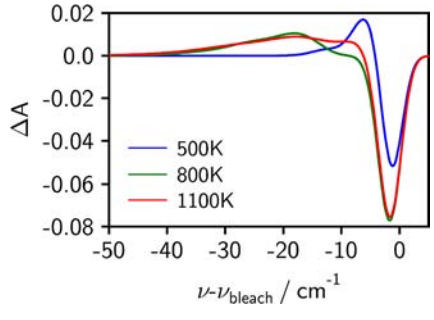

Figure 4. Calculated temperature dependence of the shape of the asymmetric C≡N stretch band of TCNE.

dx.doi.org/10.1021/ja403481v | J. Am. Chem. Soc. 2013, 135, 9843−9848

vibrational modes, whereas the bleach signal may also contain contributions due to the ion formation and is less straightforward to interpret. Therefore, the amplitude and shape of the bleach depend, in addition to the internal temperature, on the CS and CR dynamics, which control the populations of excited reactants and ion pairs. The amplitude of the positive induced absorption depends on the reaction dynamics as well. However, its shape is only related to the vibrational population; the hotter the molecule, the broader is this positive band. Figure 4 shows the simulated transient absorption band shape associated with the antisymmetric C≡N stretch of TCNE around 2200 cm^{-1} at three different temperatures (cf. Supporting Information for the details).

The spectra in Figure 3 show unambiguously that the vibrational temperature of TCNE after CR is much higher with DCA and CNPe than with MePe, indicating that in the latter case, the primary CS product is $MePe^{\bullet+}$*/$TCNE^{\bullet-}$. If the primary product was $MePe^{\bullet+}$/$TCNE^{\bullet-}$, the vibrational temperature of TCNE after CR should be as high as with DCA and CNPe.

Additionally, the low-energy side of the 2147 cm^{-1} band measured at early times is significantly broader with DCA and CNPe than with MePe. We ascribe this broadening to the vibrationally hot $TCNE^{\bullet-}$. As it is only observed with DCA and CNPe for which the CS driving force is larger than 1.2 eV, one can conclude that the effective CS driving force with MePe is substantially smaller than this value. As shown in Table 1, the latter is only possible if the primary product is $MePe^{\bullet+}$*/$TCNE^{\bullet-}$.

With DPA, the amplitudes of both the hot ground-state and the hot $TCNE^{\bullet-}$ bands are smaller than with DCA and CNPe, whereas their shapes are similar. This suggests that only a fraction of both ground-state and $TCNE^{\bullet-}$ populations are vibrationally hot and thus that both CS° and CS* are operative with DPA/TCNE.

To estimate the relative amount of energy deposited in the vibrational modes of the donors, transient IR absorption spectra were also recorded in the C=C stretch region with all four pairs (Figure 5). The observed bands are due to the donors only as the C=C stretch mode of TCNE and $TCNE^{\bullet-}$ is not IR active. The analysis of these spectra is more complicated because of the contributions of the S_1 excited state, D*, and of the radical cation, $D^{\bullet+}$, in addition to the bleach of the donor ground state and because of the weaker intensity of the bands compared to those due to the C≡N stretch. The bands associated with D* and $D^{\bullet+}$ have been identified by performing transient IR absorption measurements with all four donors alone and with MePe and CNPe only in the presence of 1 M dicyanoethylene (DCE) as acceptor (Figure S8). With DCE, CR is much slower than vibrational cooling, and thus the bands due to the hot ground state are absent from the spectra. As shown in Figure 5, hot C=C vibrations can be distinctly observed with all D/TCNE pairs as positive bands on the low-energy side of each bleach feature. With CNPe and MePe, some of these bands partially overlap with the decaying bands of the D* and $D^{\bullet+}$. Nevertheless, the continuous frequency upshift of the bands at about 1580 and 1570 cm^{-1} with CNPe and MePe is clearly visible. This shift occurs on a time scale of a few picoseconds, in good agreement with the ~5 ps time constant reported for the vibrational cooling of perylene in ACN.[22d] This complication is absent with DCA and DPA, for which the hot ground-state band shifts from ~1480 to ~1500 cm^{-1} during the first 20 ps. These results show that substantial

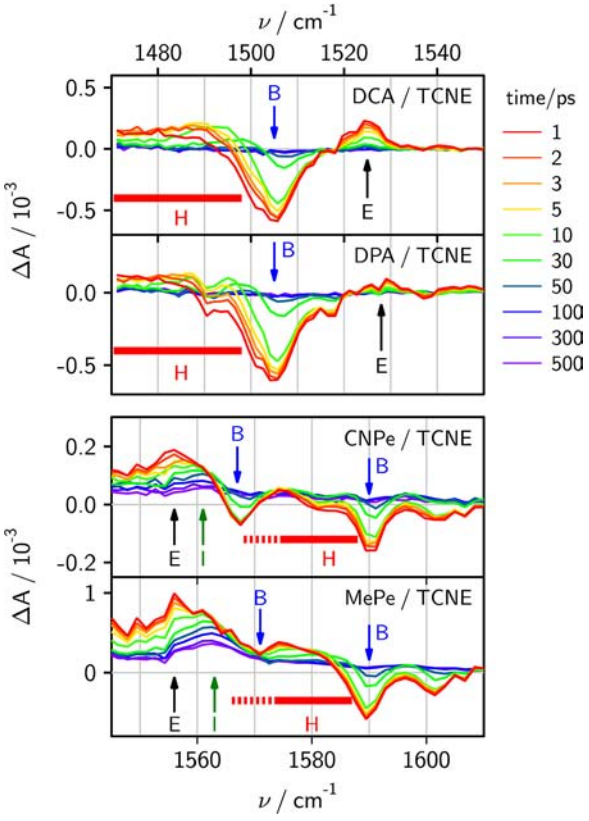

Figure 5. Transient IR absorption spectra in the C=C stretch region measured with the four D/A pairs in acetonitrile (1 M TCNE) at different time delays after 400 nm excitation (E = excited donor, I = donor radical cation, B = ground-state bleach, H = hot ground state).

energy is deposited into the vibrational modes of all four donors upon CS and CR. From these data it is, however, not possible to establish whether or not MePe is vibrationally hotter than the other donors.

Transient visible absorption measurements have been carried out to get further insight into the vibrational temperature of the donors. Figure 6 shows the resulting spectra recorded with

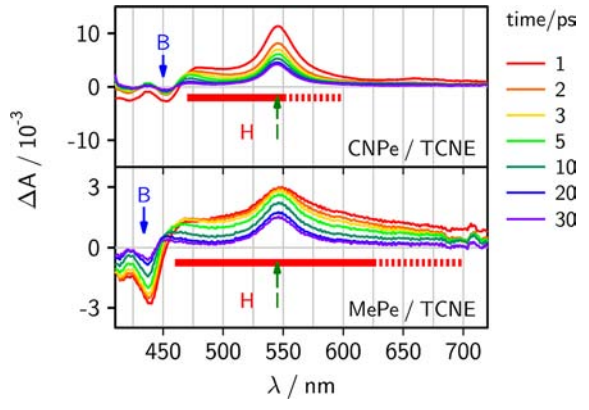

Figure 6. Visible transient absorption spectra measured with the CNPe/TCNE and MePe/TCNE pairs in acetonitrile at different time delays after 400 nm excitation (1 M TCNE). All the contributions from the donor excited state (absorption, stimulated emission, corresponding ground-state bleach) have been subtracted, leaving the ion and hot ground-state bands as well as the ground-state bleach corresponding to the ion population.

dx.doi.org/10.1021/ja403481v | J. Am. Chem. Soc. 2013, 135, 9843−9848

CNPe/TCNE and MePe/TCNE after subtraction of the bands due to the excited donor using the same procedure as for the IR spectra (Figure S5). Because of the smaller absorption coefficients of the $S_1 \leftarrow S_0$ transition of the anthracenes ($\varepsilon \sim 10^4$ vs $\sim 4 \times 10^4$ $M^{-1} \cdot cm^{-1}$ for the perylenes), the amplitude of the hot ground-state absorption is comparable to the noise. Therefore, only CNPe/TCNE and MePe/TCNE will be discussed here. The 545 nm band in the MePe/TCNE spectra is due to the $MePe^{\bullet+}$ radical cation, whereas the negative band arises from the depletion of the MePe ground-state population. The broad positive band extending from ~450 nm up to more than 700 nm at early times and narrowing on its red side during the first 10 ps can undoubtedly be ascribed to the vibrationally hot MePe ground-state population. Indeed, the electronic absorption bands of a vibrationally hot chromophore are frequency downshifted relative to those of the 'cold' chromophore when Franck−Condon active vibrational modes are thermally populated. Therefore, in a transient visible absorption spectrum, hot molecules are characterized by a positive band located on the red side of the negative ground-state bleach band.[22c,30]

This broad positive band observed with the MePe/TCNE band is totally absent with DCE as electron acceptor (Figure S6). CR of the $MePe^{\bullet+}/DCE^{\bullet-}$ pair takes place on the 500 ps time scale[31] and is thus much too slow to allow observation of the hot ground-state population. The transient visible absorption spectra measured with CNPe are similar to those with MePe and show the $CNPe^{\bullet+}$ band at 545 nm and the ground-state bleach below 470 nm. In this case, however, the positive feature due to the hot ground-state population is not as intense as with MePe and does not extend beyond 600 nm at early times, which is a straightforward evidence for the deposition of substantially more energy into the vibrational modes of MePe compared to CNPe. This result is a further support that the primary CS product with MePe/TCNE is $MePe^{\bullet+}$*/TCNE and not the ground-state ion pair.

In summary, the transient IR measurements show that, after the CS and CR processes, TCNE is vibrationally hot with DCA and CNPe but not with MePe, whereas all four donors are hot as well. Additionally, the transient visible absorption measurements reveal that substantially more energy is deposited into the vibrational modes of MePe than in those of CNPe. This is clear evidence that CS* is the predominant pathway with MePe/TCNE. Otherwise, first, TCNE would be as vibrationally hot with MePe as with the other donors, and second, MePe would not be hotter than CNPe.

This conclusion fully agrees with the relative rate constants for CS° and CS* estimated according to Marcus theory using the driving forces listed in Table 1 and assuming that the electronic coupling and the reorganization energy are the same for both processes (Figure 7). CS° with MePe is highly exergonic and is predicted to be far in the inverted region and thus to be relatively slow. On the other hand, CS* is moderately exergonic and approaches the barrierless region. As a consequence, CS* should be much faster than CS°.

Although, according to the energetics (Table 1), the same result is expected with DPA/TCNE, a non-negligible fraction of the TCNE ground-state population is vibrationally hot (Figure 3), indicating that both CS° and CS* are operative. We have only considered the first electronic excited state of the radical cations. However, the radical cation of perylene, $Pe^{\bullet+}$, has four electronic excited states below 1.95 eV.[32] As the absorption spectrum of $MePe^{\bullet+}$ is very similar to that of $Pe^{\bullet+}$, all these four

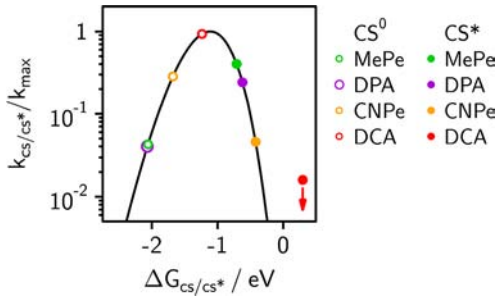

Figure 7. Driving force dependence of the ET rate constant for CS to the ground-state (open symbols) and excited (full symbols) ions estimated from Marcus theory.

states are in principle accessible upon CS*. On the other hand, the anthracene radical cation, $A^{\bullet+}$, which resembles $DPA^{\bullet+}$, has only two electronic excited states below 2 eV.[32] This different number of parallel CS* channels is probably responsible for the higher excited ion population measured with MePe.

All the results obtained with CNPe/TCNE point to CS° as the main quenching pathway, albeit CS* is energetically feasible. However, according to the estimated rate constants depicted in Figure 7, CS° is no longer in the inverted region and should thus be very fast. On the other hand, CS* is only weakly exergonic and is probably not fast enough to be competitive with CS°. Finally, CS* with DCA/TCNE is endergonic and should not be operative, in full agreement with the experimental data.

This discussion is only based on energetic considerations and presupposes that the electronic coupling, *V*, is the same for CS° and CS* in all D/A pairs investigated here. It could of course be that this is not the case, although largely dissimilar coupling energies for CS° and CS* are not expected. Despite this, as the CS rate constant depends quadratically on *V*, small differences in coupling energies could have a substantial impact on the relative efficiencies of CS° and CS*, especially if several excited states of the ionic product are accessible.

■ CONCLUSIONS AND OUTLOOK

By measuring the redistribution of the energy dissipated upon ultrafast bimolecular photoinduced CS and subsequent CR, we have been able to track the pathway of the reaction. Our results unambiguously point to the formation of excited ions when the CS to the ground-state product is highly exergonic. This is, to our knowledge, the first evidence of the involvement of excited radical ions in bimolecular photoinduced CS. As most organic radical ions have electronic excited states well below 2 eV,[21,33] the efficiency of this alternative pathway should increase as that to the ground-state product gets more exergonic and goes deeper into the inverted regime. Because of this switching of pathways, the inverted region for bimolecular photoinduced CS cannot be observed, contrary to other types of ET reactions, for which the excited states of the product are not accessible. Nevertheless, like the other ET reactions, bimolecular photoinduced CS processes can most probably be discussed in terms of Marcus theory, provided the primary product is clearly identified. Given the difficulty to recognize the presence of excited radical ions, this task is not straightforward. The approach presented here yields only qualitative information on the dominant CS pathway but does not give yet quantitative information on the relative efficiency of the various pathways. This would require a better understanding of the dissipation

dx.doi.org/10.1021/ja403481v | J. Am. Chem. Soc. 2013, 135, 9843−9848

pathways of the energy released upon CS or the identification of more direct spectroscopic signatures of excited radical ions.

■ ASSOCIATED CONTENT

Supporting Information

Experimental details, data treatment procedure, fluorescence time profiles, IR and visible spectra measured with the donors alone and with DCE, electronic absorption spectra of the donor radical cations. This material is available free of charge via the Internet at http://pubs.acs.org.

■ AUTHOR INFORMATION

Corresponding Author

nibberin@mbi-berlin.de; eric.vauthey@unige.ch

Present Addresses

[‖]Department of Physics, University of Strathclyde, 107 Rottenrow Glasgow G4 0NG U.K.

[⊥]Computational Biophysics, German Research School for Simulation Sciences, Joint venture of RWTH Aachen University and Forschungszentrum Jülich, Germany, D-52425 Jülich, Germany.

Author Contributions

[§]These authors contributed equally.

Notes

The authors declare no competing financial interest.

■ ACKNOWLEDGMENTS

This work was supported by the Fonds National Suisse de la Recherche Scientifique through project no. 200020-124393 and the NCCR MUST and by the University of Geneva.

■ REFERENCES

(1) (a) Marcus, R. A. *J. Chem. Phys.* **1956**, *24*, 966. (b) Marcus, R. A. *J. Chem. Phys.* **1965**, *43*, 679. (c) Marcus, R. A.; Sutin, N. *Biochim. Biophys. Acta* **1985**, *811*, 265.

(2) (a) Evans, M. G.; Polanyi, M. *Trans. Faraday Soc.* **1935**, *31*, 875. (b) Bell, R. P. *Proc. R. Soc. A* **1936**, *154*, 414. (c) Carey, F. A.; Sundberg, R. J. *Advanced Organic Chemistry: Part A: Structure and Mechanisms*; Springer: New York, 2007.

(3) Grampp, G. *Angew. Chem., Int. Ed.* **1993**, *32*, 691.

(4) (a) Miller, J. R.; Calcaterra, L. T.; Closs, G. L. *J. Am. Chem. Soc.* **1984**, *106*, 3047. (b) Closs, G. L.; Miller, J. R. *Science* **1988**, *240*, 440.

(5) (a) Niwa, T.; Kikuchi, K.; Matsusita, N.; Hayashi, M.; Katagiri, T.; Takahashi, Y.; Miyashi, T. *J. Phys. Chem.* **1993**, *97*, 11960. (b) Rehm, D.; Weller, A. *Isr. J. Chem.* **1970**, *8*, 259. (c) Rosspeintner, A.; Kattnig, D. R.; Angulo, G.; Landgraf, S.; Grampp, G. *Chem.—Eur. J.* **2008**, *14*, 6213.

(6) (a) Guldi, D. M.; Asmus, K. D. *J. Am. Chem. Soc.* **1997**, *119*, 5744. (b) Fukuzumi, S.; Ohkubo, K.; Imahori, H.; Guldi, D. M. *Chem.—Eur. J.* **2003**, *9*, 1585.

(7) (a) Wasielewski, M. R.; Niemczyk, M. P.; Svec, W. A.; Pewitt, E. B. *J. Am. Chem. Soc.* **1985**, *107*, 1080. (b) Chen, P.; Duesing, R.; Tapolsky, G.; Meyer, T. J. *J. Am. Chem. Soc.* **1989**, *111*, 8305. (c) Gould, I. R.; Ege, D.; Mattes, S. L.; Farid, S. *J. Am. Chem. Soc.* **1987**, *109*, 3794. (d) Mataga, N.; Asahi, T.; Kanda, Y.; Okada, T.; Kakitani, T. *Chem. Phys.* **1988**, *127*, 249. (e) Vauthey, E. *J. Phys. Chem. A* **2001**, *105*, 340.

(8) Mataga, N.; Chosrowjan, H.; Shibata, Y.; Yoshida, N.; Osuka, A.; Kikuzawa, T.; Okada, T. *J. Am. Chem. Soc.* **2001**, *123*, 12422.

(9) Rosspeintner, A.; Koch, M.; Angulo, G.; Vauthey, E. *J. Am. Chem. Soc.* **2012**, *134*, 11396.

(10) Rehm, D.; Weller, A. *Ber. Bunsen-Ges. Phys. Chem.* **1969**, *73*, 834.

(11) (a) Mataga, N. *Bull. Chem. Soc. Jpn.* **1970**, *43*, 3623. (b) Siders, P.; Marcus, R. A. *J. Am. Chem. Soc.* **1981**, *103*, 748. (c) Kikuchi, K.; Katagiri, T.; Niwa, T.; Takahashi, Y.; Suzuki, T.; Ikeda, H.; Miyashi, T. *Chem. Phys. Lett.* **1992**, *193*, 155. (d) Pagès, S.; Lang, B.; Vauthey, E. *J. Phys. Chem. A* **2004**, *108*, 549. (e) Gladkikh, V.; Burshtein, A. I.; Angulo, G.; Pagès, S.; Lang, B.; Vauthey, E. *J. Phys. Chem. A* **2004**, *108*, 6667.

(12) (a) Brunschwig, B. S.; Ehrenson, S.; Sutin, N. *J. Am. Chem. Soc.* **1984**, *106*, 6858. (b) Burshtein, A. I.; Frantsuzov, P. A.; Zharikov, A. A. *Chem. Phys.* **1991**, *155*, 91. (c) Tachiya, M.; Murata, S. *J. Phys. Chem.* **1992**, *96*, 8441.

(13) Kakitani, T.; Mataga, N. *J. Phys. Chem.* **1987**, *91*, 6277.

(14) (a) Small, D. W.; Matyushov, D. V.; Voth, G. A. *J. Am. Chem. Soc.* **2003**, *125*, 7470. (b) Vuilleumier, R.; Tay, K. A.; Jeanmairet, G.; Borgis, D.; Boutin, A. *J. Am. Chem. Soc.* **2012**, *134*, 2067.

(15) Vauthey, E. *J. Photochem. Photobiol. A* **2006**, *179*, 1.

(16) Forster, R. J.; Bertoncello, P.; Keyes, T. E. *Annu. Rev. Anal. Chem.* **2009**, *2*, 359.

(17) (a) Muller, P.-A.; Vauthey, E. *J. Phys. Chem. A* **2001**, *105*, 5994. (b) Morandeira, A.; Engeli, L.; Vauthey, E. *J. Phys. Chem. A* **2002**, *106*, 4833. (c) Nicolet, O.; Vauthey, E. *J. Phys. Chem. A* **2003**, *107*, 5894.

(18) (a) Gumy, J.-C.; Vauthey, E. *J. Phys. Chem. A* **1997**, *101*, 8575. (b) Brodard, P.; Sarbach, A.; Gumy, J.-C.; Bally, T.; Vauthey, E. *J. Phys. Chem. A* **2001**, *105*, 6594. (c) Zhao, L.; Lian, R.; Shkrob, I. A.; Crowell, R. A.; Pommeret, S.; Chronister, E. L.; Liu, A. D.; Trifunac, A. D. *J. Phys. Chem. A* **2004**, *108*, 25. (d) Grilj, J.; Laricheva, E. N.; Olivucci, M.; Vauthey, E. *Angew. Chem., Int. Ed.* **2011**, *50*, 4496. (e) Grilj, J.; Buchgraber, P.; Vauthey, E. *J. Phys. Chem. A* **2012**, *116*, 7516.

(19) Workentin, M. S.; Parker, V. D.; Morkin, T. L.; Wayner, D. D. M. *J. Phys. Chem. A* **1998**, *102*, 6503.

(20) Kikuchi, K.; Niwa, T.; Takahashi, Y.; Ikeda, H.; Miyashi, T. *J. Phys. Chem.* **1993**, *97*, 5070.

(21) Shida, T. *Electronic Absorption Spectra of Radical Ions*; Elsevier: Amsterdam, 1988; Vol. Physical Sciences data 34.

(22) (a) Elsaesser, T.; Kaiser, W. *Annu. Rev. Phys. Chem.* **1991**, *42*, 83. (b) Hamm, P.; Ohline, S. M.; Zinth, W. *J. Chem. Phys.* **1997**, *106*, 519. (c) Kovalenko, S. A.; Schanz, R.; Farztdinov, V. M.; Hennig, H.; Ernsting, N. P. *Chem. Phys. Lett.* **2000**, *323*, 312. (d) Pigliucci, A.; Duvanel, G.; Daku, L. M. L.; Vauthey, E. *J. Phys. Chem. A* **2007**, *111*, 6135. (e) Middleton, C. T.; Cohen, B.; Kohler, B. J. *Phys. Chem. A* **2007**, *111*, 10460. (f) Benniston, A. C.; Matousek, P.; McCulloch, I. E.; Parker, A. W.; Towrie, M. *J. Phys. Chem. A* **2003**, *107*, 4347.

(23) Vauthey, E.; Högemann, C.; Allonas, X. *J. Phys. Chem. A* **1998**, *102*, 7362.

(24) (a) Elles, C. G.; Cox, M. J.; Crim, F. F. *J. Chem. Phys.* **2004**, *120*, 6973. (b) Rosspeintner, A.; Lang, B.; Vauthey, E. *Annu. Rev. Phys. Chem.* **2013**, *64*, 247.

(25) Burshtein, A. I. *Adv. Chem. Phys.* **2004**, *129*, 105.

(26) (a) Mohammed, O. F.; Banerji, N.; Lang, B.; Nibbering, E. T. J.; Vauthey, E. *J. Phys. Chem. A* **2006**, *110*, 13676. (b) Mohammed, O. F.; Adamczyk, K.; Banerji, N.; Dreyer, J.; Lang, B.; Nibbering, E. T. J.; Vauthey, E. *Angew. Chem., Int. Ed.* **2008**, *47*, 9044.

(27) Horng, M. L.; Gardecki, J. A.; Papazyan, A.; Maroncelli, M. *J. Phys. Chem.* **1995**, *99*, 17311.

(28) Nibbering, E. T. J.; Fidder, H.; Pines, E. *Annu. Rev. Phys. Chem.* **2005**, *56*, 337.

(29) Keane, P. M.; Wojdyla, M.; Doorley, G. W.; Watson, G. W.; Clark, I. P.; Greetham, G. M.; Parker, A. W.; Towrie, M.; Kelly, J. M.; Quinn, S. J. *J. Am. Chem. Soc.* **2011**, *133*, 4212.

(30) (a) Grilj, J.; Zonca, C.; Daku, L. M. L.; Vauthey, E. *Phys. Chem. Chem. Phys.* **2012**, *14*, 6345. (b) Petersson, J.; Eklund, M.; Davidsson, J.; Hammarström, L. *J. Phys. Chem. B* **2010**, *114*, 14329.

(31) Pagès, S.; Lang, B.; Vauthey, E. *J. Phys. Chem. A* **2006**, *110*, 7547.

(32) Hirata, S.; Lee, T. J.; Head-Gordon, M. *J. Chem. Phys.* **1999**, *111*, 8904.

(33) Shida, T.; Iwata, S. *J. Am. Chem. Soc.* **1973**, *95*, 3473.